

1
2 Importance of Mobile Genetic Element Immunity in Numerically Abundant *Trichodesmium* Clades
3
4
5
6
7
8
9

10 Eric A. Webb^{1*}, Noelle A. Held^{2,3#}, Yiming Zhao¹, Elaina Graham¹, Asa E. Conover¹, Jake Semones¹,
11 Michael D. Lee⁴, Yuanyuan Feng⁵, Feixue Fu¹, Mak A. Saito², David A. Hutchins¹
12
13
14
15
16
17
18
19
20
21
22

23 ¹ Marine and Environmental Biology, Department of Biological Sciences, University of Southern
24 California, Los Angeles, CA 90089, USA

25 ² Department of Marine Chemistry and Geochemistry, Woods Hole Oceanographic Institution, Woods
26 Hole, MA 02543, USA

27 ³ Department of Earth, Atmospheric, and Planetary Sciences, Massachusetts Institute of Technology,
28 Cambridge, MA 02139, USA

29 ⁴ Blue Marble Space Institute of Science, NASA Ames Research Center, Mountain View, CA 94035, USA

30 ⁵ College of Marine and Environmental Sciences, Tianjin University of Science and Technology, Tianjin
31 300457, China

32 [#] Present address: Department of Environmental Systems Science, ETH, Zurich, Switzerland
33
34
35
36
37
38
39
40
41
42

43 *Correspondence: Eric A. Webb (eawebb@usc.edu)
44
45

46 Running Title: CRISPR-Cas in *Trichodesmium*
47

1 **Abstract**
2

3 The colony-forming cyanobacteria *Trichodesmium* spp. are considered one of the most important
4 nitrogen-fixing genera in the warm, low nutrient, open ocean. Despite this central biogeochemical role,
5 many questions about their evolution, physiology, and trophic interactions remain unanswered. To
6 address these questions, we describe the genetic potential of the genus via significantly improved
7 genomic assemblies of strains *Trichodesmium thiebautii* H94, *Trichodesmium erythraeum* 2175, and 17
8 new *Trichodesmium* metagenome-assembled genomes (MAGs, >50% complete) from hand-picked,
9 *Trichodesmium* colonies spanning the Atlantic Ocean. Phylogenomics identified ~four N₂ fixing clades of
10 *Trichodesmium* across the transect, with *T. thiebautii* dominating the colony-specific reads. Pangenomic
11 analyses showed that all *T. thiebautii* MAGs are enriched in defense mechanisms and encode a vertically
12 inherited Type III-B Clustered Regularly Interspaced Short Palindromic Repeats and associated protein-
13 based immunity system (CRISPR-Cas hereafter). Surprisingly, this CRISPR-Cas system was absent in all
14 *T. erythraeum* genomes and MAGs, vertically inherited by *T. thiebautii*, and correlated with increased
15 signatures of horizontal gene transfer. Multiple lines of evidence indicate that the CRISPR-Cas system is
16 functional in situ: 1. *Trichodesmium* CRISPR spacer sequences with 100% identical hits to field-
17 assembled, putative phage genome fragments were identified, 2. High *Trichodesmium* spacer sequence
18 variability indicating rapid adaptation, and 3. metaproteomic and transcriptomic expression analyses
19 detecting the CRISPR-Cas system components in *Trichodesmium* colonies from the Atlantic and Pacific
20 Oceans. These data suggest that phage or mobile genetic element immunity in *T. thiebautii* could
21 contribute to their success, gene diversity, and numerical dominance over *T. erythraeum* in the oceans,
22 thus warranting further *Trichodesmium* virome investigations.

23

1 **Significance statement**

2 Our work identifies CRISPR-Cas immunity as a phylogenetically distinct, environmentally expressed
3 factor in the speciation of closely related N₂-fixing *Trichodesmium* clades. These findings suggest that
4 differential phage predation and resistance could be a previously overlooked selective pressure in the
5 genus, potentially leading to the current numerical dominance of *T. thiebautii* over *T. erythraeum* in the
6 oceans. Furthermore, while the currently CO₂-limited *T. erythraeum* is expected to be a 'winner' of
7 anthropogenic climate change, their predicted higher phage sensitivity than *T. thiebautii* could challenge
8 this outcome.

9

10

1 Low bioavailable concentrations of nitrogen can limit primary productivity in many oceanic
2 euphotic zones (e.g., (1)). In the warm, oligotrophic open ocean, these low nitrogen concentrations select
3 for nitrogen-fixing organisms that can efficiently convert atmospheric N₂ to bioavailable NH₄ or amino
4 acids (2). While our understanding of nitrogen-fixing organisms in the oceans is evolving to include non-
5 autotrophic diazotrophs and other unexpected physiologies (e.g., (3–5)), the filamentous, colony-forming
6 cyanobacterium *Trichodesmium* is still considered a critical oceanic nitrogen fixer (3, 6).

7 Mariners have known filamentous *Trichodesmium* spp. as 'sea-saw dust' for hundreds of years
8 because of the massive surface blooms they can form resembling small, water-suspended wood
9 shavings (6). *Trichodesmium* filaments can aggregate in natural communities, forming 1–4 mm colonies of
10 essentially two morphologies (i.e., radial tufts or spherical puffs; (7)) that are visible to the naked eye and
11 thus aided these early observations. Fitting with this long-term recognition, botanical scientists defined six
12 morphologically described species as early as the late 1800s (8). Still, oceanographers did not recognize
13 their central role in N₂ fixation until the 1960s ((2, 3)4/20/2022 2:17:00 PM and references therein).

14 Researchers now know that *Trichodesmium* has a wide distribution in the tropics and subtropics (3, 9)
15 and, even though some appear to have lost N₂ fixation capabilities (5), the genus is still an essential
16 source of bioavailable N to the oligotrophic oceans (6, 10, 11). Thus, while *Trichodesmium* species
17 names have existed for >100 years, experiments to understand their evolution, genomic potential, and
18 ecological impact are still active research areas.

19 Members of the *Trichodesmium* genus are closely related. Yet, enrichment strains and field
20 samples can show surprising morphological and physiological character variability (i.e., pigmentation, cell
21 size, trichome shape, growth rate, N₂ fixation rate, or colony structure) and abundance differences (e.g.,
22 (7, 12–15)). For example, marker gene phylogenetics shows four clades of *Trichodesmium* (7, 12, 16),
23 with the best bootstrap support defining the *Trichodesmium thiebautii* and *Trichodesmium erythraeum*-
24 enriched clades I and III, respectively (7). Additionally, morphological and molecular fieldwork shows that
25 members of these same two clades are commonly observed and that *T. thiebautii*-containing clade I is
26 typically more abundant throughout the water column (e.g., (5, 9, 13, 17, 18)). Thus, while there are six
27 classically defined *Trichodesmium* species of varying pigmentation colors and sizes, *T. thiebautii* typically

1 dominates the in situ community. Despite this recognition, the internal and external factors causing the
2 numerical dominance of *T. thiebautii* are poorly defined.

3 Herein we used metapangenomics and metaproteomics of enrichment cultures and hand-picked
4 *Trichodesmium* colonies spanning the Atlantic Ocean to define *T. thiebautii* genomic features that help to
5 explain their population dynamics among *Trichodesmium* communities. Our efforts show that predicted
6 mobile genetic element immunity (i.e., against phage and mobile plasmids) is a defining feature of *T.*
7 *thiebautii*, as all clade members maintain and express a conserved Type III-B CRISPR-Cas system (19).
8 Many of the *T. thiebautii* CRISPR-Cas spacers matched phage genome fragments assembled from same
9 cruise samples. Thus, differential phage resistance could help explain the current numerical abundance
10 of *T. thiebautii* over *T. erythraeum*. This result also raises questions about the likelihood of *T. erythraeum*
11 displacing *T. thiebautii* as climate changes (14, 20).

12

13 **Results and Discussion**

14 **All N₂-fixing *Trichodesmium* genomes are ‘low’ protein-encoding.** Past work with a handful of
15 *Trichodesmium* isolates shows that their genomes are low protein-encoding (i.e., ~63%) and enriched in
16 selfish DNA elements (21); however, these observations have never been studied systematically across
17 the genus. To address this, we assembled 17 new *Trichodesmium* MAGs from our hand-picked colonies
18 obtained on the 2018 Atlantic Ocean spanning TriCoLim cruise (**Materials and Methods, Fig. 1**) and
19 compared them to previously published isolate genomes (21) and four MAGs from a Tara Oceans
20 analysis (5). Two of our previously published USC *Trichodesmium* Culture Collection (USCTCC)
21 genomes, *T. thiebautii* H94 and *T. erythraeum* 2175, were significantly improved by MiSeq resequencing
22 the former and Anvi'o refining both using reads from TriCoLim. **Supp. Table 1** lists the final refined
23 CheckM (22) statistics for all MAGs and genomes, data that more than doubles the genomic information
24 available for this important genus.

25 Similar to the three isolate comparison by Walworth et al. (21), **Supp. Table 2** shows that
26 *Trichodesmium* MAGs >50% complete have low GC% (35 ± 1%) and much lower coding (64 ± 4%) than
27 the bacterial average of ~90% (23). Because MAG fragmentation and lower completeness scores can
28 significantly change many genome stats, we also calculated these values in higher quality MAGs (i.e.,

1 >80% complete). Our subset obtained a similar coding percentage from above ($63 \pm 4\%$) but more
2 consistent values for other parameters. Specifically, *Trichodesmium* genomes are large, with an average
3 length of $\sim 6.5 \pm 0.9$ MB, and relatively gene sparse, only encoding for an average of $\sim 5396 \pm 784$
4 proteins.

5 **There are four N₂-fixing clades of *Trichodesmium*.** Even though *Trichodesmium* spp. were initially
6 described in the late 1800s, their phylogenetic relationships are still being developed. For example,
7 research using one to three genes has shown that *Trichodesmium* genus members are distributed in two-
8 to-four clades. However, much of the inferred tree topology in those studies was lower support (7, 12, 24).
9 To improve *Trichodesmium* cladistics, we performed phylogenomics using 251 conserved core genes
10 from *Trichodesmium* genomes and MAGs >50% complete. The resulting tree in **Fig. 2A** shows that the
11 N₂-fixing members of the genus are divided into four major clades. While the tree will likely be improved
12 by including more taxa to resolve subclade structure, it also needs more isolate genomes or MAGs from
13 other oceanic basins (i.e., only three MAGs were from outside of the Atlantic). That said, while all
14 *Trichodesmium* MAGs are very closely related by average nucleotide identity (>88% ANI), the tree
15 suggests that the *T. thiebautii* assembled from the Atlantic (Clade A) are phylogenomically different from
16 those from other basins (Clade B). However, our read recruiting and metaproteomics (see below) indicate
17 that genomes with high identity to *T. thiebautii* B are also present and active in the Atlantic Ocean, but
18 they did not assemble with high quality from TriCoLim samples (e.g., **Supp Table 1**; St11_bin2_1_1 and
19 St14_bin2_1 are >98% ANI with *T. thiebautii* B H94 and MAG_ *Trichodesmium thiebautii*_Indian). Lastly,
20 while Delmont has shown that some clades of *Trichodesmium* are non-N₂-fixers (5), BLAST searches of
21 the TriCoLim MAGs with *T. erythraeum* IMS101 *nif* genes confirmed that all of these MAGs likely encode
22 for diazotrophy (i.e., when missing in a MAG annotation, *nif* genes were consistently found as gene
23 fragments at the end of contigs).

24 Since there are no published isolate genomes for *T. thiebautii* clade A and *T. erythraeum* clade B,
25 reconciling the past species designations and predicting their physiological and morphological characters
26 was not directly possible. However, we attempted to place these MAGs in context with previously isolated
27 strains by comparing their 16S-23S internal transcribed spacer (ITS) gene sequences with prior
28 *Trichodesmium* enrichment diversity studies (7, 24) via blast. We chose the ITS sequence because past

1 researchers have commonly used this DNA region to probe the diversity and abundance of closely
2 related cyanobacteria (e.g., (25–27)). The isolate ITS hits ranged from 86-100% ID to our MAGs and
3 tracked well with our cladistics. However, the high identity hits (>99.5% ID) allowed us to make three
4 conclusions. **1.** The ITS does not contain enough information to determine if previous *Trichodesmium*
5 *hildebrandtii*, *Trichodesmium tenue*, and *Trichodesmium spiralis* isolates are in either *T. thiebautii* clade A
6 or B. **2.** *Trichodesmium contortum* with substantial diameter cells (~20-30 μ m) and bright red coloration is
7 likely a member of *T. erythraeum* clade A. **3.** *T. erythraeum* strains (6-1, 6-2, 6-5) that formed a weak
8 subgroup in a prior analysis (7) are members of *T. erythraeum* clade B. Thus, based on Hynes et al.,
9 2012 we predict that *T. erythraeum* clade B members are phycoerythobilin-rich red cells ~6.5-9.5 μ m in
10 diameter that can form colonies or loose aggregates. However, more isolate genomes are needed to
11 connect the varied morphologies and pigments observed in *T. thiebautii*, *T. hildebrandtii*, and *T. tenue*
12 isolates (7) with our phylogenomics. Thus, hereafter we forgo using other *Trichodesmium* species names
13 and simply use the broad clade designations (i.e., *T. erythraeum* A & B and *T. thiebautii* A & B).

14 ***Trichodesmium* genomes have many paralogous genes dominated by predicted mobile genetic
15 elements.** To understand broad-level genome evolution in the genus, we explored copy number enriched
16 gene families in *Trichodesmium* genomes and MAGs. To accomplish this, we imported each assembly
17 into the Anvio'o pangenomic interface (28, 29), segregated prodigal predicted genes into gene clusters
18 (GCs) with BLAST (30, 31), and annotated these GCs with the 2020 COGs (32) and PFAM (33) datasets.

19 Our results show many paralogous GCs shared by all *Trichodesmium* genomes, with some found
20 in very high copy numbers per clade. Interestingly, each clade's top ten duplicated GCs are similar but not
21 100% identical in sequence or copy number (**Supp. Table 3**). The predicted annotation of these GCs
22 shows that they are enriched (~78%) in selfish DNA elements like transposases or retrons. For example,
23 GC_00000001 (predicted to be a transposase) is present in 10 of the 13 genomes at 327 copies but is
24 heavily enriched in *T. erythraeum* A MAGs (i.e., MAG_*Trichodesmium erythraeum* and St11_bin5). One
25 other GC shared by all *Trichodesmium* clades found in high copy numbers was GC_00000002. This GC
26 is annotated as 'Retron-type reverse transcriptase' and comprises 342 genes found in as high as 38
27 copies per genome. Our annotation predicts that this retron is part of a group II self-splicing intron. While
28 the fundamental roles of retrons and group II introns in microbiology are still developing, there is some

1 evidence that they can be involved in bacterial genome re-arrangement or niche adaptation (34–37). Both
2 GC_00000003 (annotated as ‘Transposase|CRISPR-associated protein Csa3, CARF domain (Csa3)’)
3 and GC_00000004 (annotated as ‘Transposase’) are >3-times copy number enriched in *T. thiebautii*
4 clades compared to *T. erythraeum*. Finally, the most abundant duplicated GC in *T. erythraeum* B,
5 GC_00000008 (predicted to be a transposase), is ~>20 times more abundant in this clade compared to
6 others that maintain it, and it is absent from *T. thiebautii* B. While the factors causing these
7 enrichments/depletions are not defined, these data corroborate a prior finding that *Trichodesmium*
8 genomes are repeat-rich (21) and show that these duplications are commonplace in situ. Furthermore, as
9 seen elsewhere (e.g., (38, 39)), these results suggest that transposition or other related duplication
10 generating processes are important evolutionary mechanisms in *Trichodesmium*.

11 ***T. thiebautii* MAGs are enriched in specific clusters of orthologous genes (COG) compared to *T.***
12 ***erythraeum***. To begin to understand the selective pressures driving speciation in the genus, we next
13 characterized the genomic potential of *Trichodesmium* in a phylogenomic context. At first glance, the
14 average gene number per genome is greater in *T. thiebautii* than *T. erythraeum* (**Supp. Tables 4-7**). We
15 used the Anvi’o pangenomic interface (28, 29) described above to characterize these differences,
16 combined with R graphing and statistics. As shown in **Fig. 2B**, many of the COG categories per 100kb in
17 each clade are statistically indistinguishable by ANOVA. However, there are five enriched categories in *T.*
18 *thiebautii* A, *T. thiebautii* B, or both. These include Lipid Metabolism (I), Intracellular trafficking (U),
19 Defense Mechanisms (V), Mobilome (X), and genes not categorized by COG.

20 Closer inspection of the COG categories enriched can give more insight into clade-specific niche
21 adaptation. Specifically, the Lipid Metabolism COGs show that *T. thiebautii* A has increased acyl-carrier
22 proteins, many of which appear to be involved in polyketide synthases or annotated with multiple
23 functions. These findings suggest increased secondary metabolite production in this clade. Independent
24 analysis with the secondary metabolite prediction software antiSMASH (40) on the same 13
25 *Trichodesmium* assemblies also predicted that *T. thiebautii* makes specialized compounds. These include
26 compounds similar to the cancer cell toxin Curacin A (41) and the hydrocarbon 1-heptadecene (42).
27 However, despite the interest in understanding how *Trichodesmium* acquires Fe (e.g., (15, 43, 44)), no
28 putative siderophore producing clusters were defined by antiSMASH. The Intracellular Trafficking COGs

1 enriched in *T. thiebautii* are mostly large repeat-rich proteins (i.e., annotated as predicted “CHAT
2 domains,” “haemagglutination activity domain,” or “tetratricopeptide repeats”), those implicated in
3 attachment, and related to secretory pathways. However, select BLAST analyses showed that many of
4 these proteins’ closest hits are conserved hypotheticals (typically in other cyanobacterial genomes).
5 Putative transposases or related genes were heavily enriched in the Mobilome, Defense, and non-
6 categorized COG categories. NCBI nr BLAST searches showed that hypothetical proteins were also
7 prevalent in non-categorized COG categories gene clusters. The *T. thiebautii* Defense category was
8 enriched in putative toxin-antitoxin proteins (45–47) antiphage systems defined in (48), and CRISPR-Cas
9 genes (19, 49).

10 **One-quarter of all *Trichodesmium* MAGs have shared gene clusters.** To more closely explore
11 differences between *Trichodesmium* clades, we examined specific gene cluster presence/absence,
12 annotated function (i.e., via COG function, COG pathway (32), PFAM (33), KOFAM (50) and KEGG (51))
13 and detection in our TriCoLim reads. This effort allowed us to determine if the functionalities enriched or
14 depleted in each clade in **Fig. 2B** were caused by distinct, new gene clusters, paralogous duplications, or
15 deletions. Additionally, the GC matrix generated by Anvi'o allowed us to characterize the existing
16 *Trichodesmium* pangenome and determine its genome fluidity (52).

17 Our metapangenomic analysis used one closed *Trichodesmium* genome (i.e., *T. erythraeum*
18 IMS101; (21)) and twelve MAGs >80% complete and is shown in **Fig. 3**. As seen before (53, 54), our data
19 support the supposition that tuft and puff colony morphology does not correlate with specific clades of
20 *Trichodesmium*, as *T. thiebautii* assemblies dominated the read recruiting regardless of hand-picked
21 sample colony morphology (**Fig 3B**; black heat map). Intra-clade average nucleotide identity (ANI) of the
22 MAGs was very high. Thus, in situ quantification of each was not possible because of likely random read
23 recruiting among high ANI genomes (55). However, since this issue would likely only underestimate the
24 abundances of each clade, we report that *T. thiebautii* MAGs were recruiting at least 1-2 orders of
25 magnitude more reads than *T. erythraeum* from TriCoLim colonies.

26 Next, we sought to understand the minimum and maximum genetic potential encoded in
27 *Trichodesmium* genomes. Based on the BLAST clustering, there are 1454 blast-derived, single and

1 paralogous GCs in the conservative *Trichodesmium* core found in all genomes (**Fig. 3A**). Thus,
2 approximately 1/4 of each genome is conserved core gene content. The total pangenome count was
3 10,054 genes. Pangenome modeling with the R package micropan (56) obtained Heap's power law alpha
4 estimates of ~1 for all *Trichodesmium* MAGs together and slightly >1 for *T. thiebautii* and *T. erythraeum*
5 MAGs individually, indicating that these pangenomes are either 'completely' sampled with this dataset
6 (i.e., closed) or slowly growing logarithmically (57).

7 Others have argued that genome fluidity (\square), a metric of genome dissimilarity, is a better method
8 for estimating the likelihood of identifying new genes as more genomes in a group are sequenced (52,
9 58). We determined the MAG genome fluidity values for all *Trichodesmium* ($\square = 0.303 \pm 0.10$) and the
10 major clades of *T. thiebautii* ($\square = 0.24 \pm 0.04$), and *T. erythraeum* ($\square = 0.18 \pm 0.03$). Strict interpretation of
11 these data suggests a 30% chance of identifying new genes as more *Trichodesmium* genomes are
12 sequenced – again fitting with a growing/open pangenome. While it is important to note that these \square
13 values will likely improve with increased numbers of genomes in each clade (52), the data are consistent
14 with the *T. thiebautii* pangenome being more 'open' than *T. erythraeum* and likely experiencing increased
15 horizontal gene transfer (HGT) incorporation rates than the former.

16 ***Trichodesmium* auxiliary gene content and genomic average nucleotide identity (ANI) recapitulate**
17 **the phylogenomic signal.** While the predicted *Trichodesmium* core N₂-fixing genome makes up ~1/4 of
18 the genes, many auxiliary GCs are also detected. As shown in **Fig. 3A**, some auxiliary GCs were only
19 found in one genome (i.e., singletons), while others associate with specific clades. The environmentally
20 accessory genes (EAGs; i.e., not found in situ) to environmentally core genes (ECGs; i.e., found in situ)
21 ratio shown on the outer ring indicates that many, but not all of these auxiliary GC bins, are commonly
22 detected in Atlantic Ocean *Trichodesmium* colonies. Coloring the rings of **Fig. 3A** by phylogenomic group
23 shows that the auxiliary gene content, average nucleotide identity (ANI; **Fig. 3B**), and phylogenomics of
24 core genes (**Fig 2A**) give the same relationships between *Trichodesmium* clades. Additionally, statistical
25 analysis of the singleton genes shows an uneven distribution in the genus, with *T. thiebautii* genomes
26 maintaining significantly more (**Fig. 3C**). These empirical data are consistent with the genome fluidity
27 results above and suggest mechanisms that increase novel gene content, like horizontal gene transfer,
28 are more common in *T. thiebautii*.

1 We next took the GCs in each clade-specific bin, highlighted in **Fig. 3A**, to characterize enriched
2 functionalities. The largest groups of clade-specific genes are found in the primary division between *T.*
3 *thiebautii* AB and *T. erythraeum* AB, where the former shares 313 GCs and the latter shares 315,
4 respectively. Other clear GC groupings were observed in *T. erythraeum* B (198 GCs), *T. erythraeum* A
5 (118 GCs), and *T. thiebautii* B (114 GCs). We performed percentage normalized COG analyses of these
6 conserved GC bins (**Supp. Fig. 1**), and this effort showed four things: **1.** Non-COG categorized GCs
7 dominate those found in all bins (ranging from ~44 to 79%), and 18-75% of these non-categorized GCs
8 are hypotheticals based on BLAST searches against NCBI nr (2021-03-01 version), **2.** The Tery-AB bin
9 has much more COG diversity than the similarly sized Thieb bin (315 and 313 GCs, respectively), **3.**
10 Thieb, Thieb-B, and Tery-B bins are enriched in mobilome sequences (~10% of the bin's GCs), while in
11 Tery-A and Tery-AB, the mobilome GCs only account for ~5% of GCs, and **4.** The Thieb bin has a higher
12 percentage of Defense COGs. While our data show that specific CRISPR-related gene duplications are
13 common in *Trichodesmium* MAGs (Duplicated GCs; **Supp. Table 3**), the Thieb-specific bin is enriched in
14 CRISPR-Cas immunity genes.

15 ***T. thiebautii* encodes a complete Type III-B CRISPR-Cas system, while *T. erythraeum* does not.** To
16 more rigorously characterize and identify the CRISPR-Cas system in *Trichodesmium*, we scanned all
17 assemblies with CRISPRCasTyper (59). This tool aids in the sometimes difficult task of identifying and
18 typing CRISPR arrays and disparate *cas* loci based on the currently defined 44 subtypes and variants
19 (19). The expanded phylogenomic tree in **Fig. 4A** shows a graphical representation of *cas* gene detection
20 and indicates that all *T. thiebautii* assemblies, and those from nearest phylogenomically-defined relatives
21 (*i.e.*, specific *Okeania* and *Hydrocoleum* MAGs), are predicted to encode CRISPR-Cas systems (*e.g.*,
22 comprised of >15 genes in *T. thiebautii* H94). At the same time, none of the 13 assembled *T. erythraeum*
23 MAGs or enrichment genomes have them. Importantly, since the Joint Genome Institute closed the *T.*
24 *erythraeum* IMS101 genome (21), the complete absence of a CRISPR-Cas system in this strain supports
25 that they are also missing from *T. erythraeum* MAGs and, not coincidentally in the gaps of a fragmented
26 MAG.

27 As the *cas10* gene is diagnostic for the Type III-B CRISPR predicted to be encoded by *T.*
28 *thiebautii* and can show significant sequence variation (49), we performed phylogenetic analyses of

1 Cas10 protein sequences to explore the origins of this system in the lineage (**Fig 4A**). The Cas10
2 maximum likelihood phylogeny shown in **Fig. 4B** suggests two-to-three Type III-B systems in *T. thiebautii*.
3 Additionally, this tree indicates that these systems are likely ancestral because the phylogeny of each of
4 the three distinct sequence clusters is roughly congruent with the phylogenomic signal shown in **Fig. 4A**.
5 However, careful comparison of both trees shows that all three Type III-B Cas10 protein clusters are not
6 conserved in every *T. thiebautii* assembly. 'Missing' *cas10* genes lost in assembly gaps or actual deletion
7 of one or more clusters in that MAG could cause this discrepancy. BLASTN searches confirmed that the
8 missing *cas10* genes were present at contig breaks in our *T. thiebautii* MAGs (i.e., St18_bin1, St19_bin1,
9 and St16_bin2_tuft) corresponding to clusters 1 & 2 in **Fig. 4B**. We could not identify any additional gene
10 fragments for cluster 3 or hits in *T. erythraeum* MAGs. The most straightforward interpretation of these
11 data is that most *T. thiebautii* assemblies do not have cluster 3, and perhaps it is currently disappearing
12 from the *Trichodesmium* pangenome. Fittingly, cluster 3 is undetectable from our best-assembled MAG,
13 *T. thiebautii* H94 isolate genome (566 contigs). Thus, unlike the commonly observed stochastic
14 presence/absence of CRISPR-Cas systems in closely related bacteria (e.g., (60–63), the loss of the III-B
15 CRISPR-Cas system in *T. erythraeum* is phylogenetically constrained and is a defining difference
16 between the major clades of the genus.

17 Generally speaking, CRISPR-Cas systems protect the cell from mobile genetic elements (MGEs;
18 phage and mobile plasmids) via a sequence-based, targeted genome degradation (60, 64). Many
19 different CRISPR-Cas systems that vary in gene content and recognition molecule (RNA vs. DNA) have
20 been described (19). That said, while all CRISPR-Cas variants appear to provide memory-driven
21 immunity against MGEs, the Type III-B subtype, predicted in numerically abundant *T. thiebautii* clades,
22 requires active RNA transcription for function, can use other CRISPR arrays in addition to its own and
23 provides better protection against phage protospacer mutagenic evasion (65).

24 Mechanistically, Type III-B CRISPR-Cas systems operate in three steps **1**. Adaptation:
25 recognition and incorporation of transcribed 30-50bp protospacers (i.e., DNA or RNA sequences of
26 invading MGEs; typically mediated by Cas1 or Cas1-reverse transcriptase (RT) fusion proteins,
27 respectively (66, 67)) into CRISPR arrays as spacer sequence DNA 'memories' of past attacks, **2**.
28 Expression: spacer RNAs are expressed as precursor CRISPR RNA (crRNA), and **3**. Interference:

1 sequence-specific crRNAs guides interfere with invading phage or plasmids by the action of the Cas10
2 protein (49, 60). The absence of a Cas1-RT fusion protein in *T. thiebautii* suggests that the primary
3 adaptation targets for this system are DNA MGEs. In contrast, an HD superfamily nuclease domain in *T.*
4 *thiebautii* Cas10 proteins indicates that the interference step is likely cleaving both RNA and transcribed
5 DNA (49, 66, 68). Importantly, these DNA spacer sequences also provide ‘fingerprints’ of past MGE
6 attacks that link phage/plasmid sequences with the CRISPR-Cas system containing host (e.g., (69–74)).

7 **Predicted phage genome fragments assembled from TriCoLim 100% match *T. thiebautii* CRISPR
8 spacers.** We next sought to identify predicted MGEs from colony assemblies and determine if they
9 matched *T. thiebautii* spacer sequences. To accomplish this, we asked if putative phage genomes were
10 detectable in our assemblies (*i.e.*, from enrichment cultures and TriCoLim) using virsorter2 and DRAM-V
11 (75, 76), and we attempted to assemble plasmids using metaplasmidSPAdes (77). While
12 metaplasmidSPAdes identified several putative plasmids in enrichment and field samples (data not
13 shown), none matched any *T. thiebautii* spacers. We also could not detect phage particles/genomes from
14 the enrichment MAGs; however, the TriCoLim assemblies revealed 1000s of putative phage genome
15 fragments with contigs sizes ranging from 1000s to >100kbps (data not shown).

16 Next, we asked whether these putative phage genomes had sequences matching the *T. thiebautii*
17 spacers using *Trichodesmium* spacer blast searches against the complete DRAM-V predicted phage
18 genomes dataset. This effort identified seven 100% ID hits and 29 more with ANI >90% covering $\geq 93\%$
19 of the spacer (**Supp. Table 8**). We conservatively picked the latter ID and coverage level because Type
20 III-B crisper systems can function with mismatches, a feature that requires phage to delete ‘whole’
21 spacer-protospacer targets from their genomes to escape degradation (78–80). Unfortunately, these
22 spacer-matching putative phage DNA fragments only ranged from 1763 to 5636 bps and were thus too
23 small to identify the phage. All spacer-matching contigs were categorized as virsorter2 category 2 (*i.e.*,
24 likely phage DNA) and contained many predicted hypothetical viral genes, while one also is expected to
25 encode a transposase (**Supp. Table 9**). It is noteworthy that many of these putative phage genome
26 fragments were detected multiple times from independently assembled TriCoLim stations (**Supp. Table 9**;
27 **fastANI groupings**), suggesting that some consistent phage particles were present across the transect.
28 As past research shows that high phage relatedness selects for CRISPR-Cas systems (60, 81, 82), these

1 data suggest that the *T. thiebautii* CRISPR-Cas system is defending against a relatively conserved phage
2 group.

3 ***T. thiebautii* CRISPR-Cas systems are expressed in situ.** Identifying conserved *Trichodesmium*
4 spacers and putative phage genome fragments suggests that the CRISPR-Cas systems are active in the
5 field. To verify, we screened our TriCoLim *Trichodesmium* colony metaproteomics dataset for in situ Cas
6 protein expression. We used non-identical predicted protein sequences from each *Trichodesmium*
7 genome and MAG in **Fig. 3A** as a protein database to screen environmental *Trichodesmium* colony
8 peptide mass spectral data (83). In this re-analysis, we identified 3498 proteins and 68058 peptides. After
9 binning the detected proteins by clade, *T. thiebautii* proteins were >10x more abundant across the
10 transect than either *T. erythraeum* clades (**Fig. 5a** - Red, Pink, Blue, and Cyan filled colored bars,
11 respectively). This protein detection dataset agrees well with our metagenomic read mapping in **Fig. 3B**,
12 where *T. thiebautii* consistently dominated the sequencing reads. Major metabolic proteins such as the
13 photosystems and nitrogenase were detected in high levels across the transect (**Fig. 5B**) and originated
14 mainly from *T. thiebautii* proteins. Non-COG categorized proteins were 50x more abundant across the
15 transect than even these core metabolic functions, consistent with this being one of the most enriched
16 categories in the *T. thiebautii* assemblies. Additionally, the in situ expression of these non-categorized
17 proteins suggests that they are required for environmental growth and highlights the importance of
18 characterizing them further.

19 Proteins involved in cellular defense, including toxin/antitoxin proteins (*i.e.*, the toxin components
20 of RelE and MazEF and the antitoxin component of ParD) and the CRISPR-Cas system, were identified
21 in appreciable abundance across the transect (**Fig. 5C**). The CRISPR-Cas proteins did not correlate with
22 total *T. thiebautii* protein abundance, suggesting that the former are not constitutively expressed (*i.e.*, as a
23 function of biomass) and are instead under some regulatory control. The CRISPR proteins identified
24 included Cas10 and Cas7, and their phylogenetic assignment at the peptide level corresponded to *T.*
25 *thiebautii* species and were assigned Cas10 clusters 1 & 2 from **Fig. 4B**. Specifically, we identified
26 peptides that were identical to those in *T. thiebautii* MAGS H94, St18_bin1, St16_bin2, and MAG *T.*
27 *thiebautii* Indian Ocean, indicating that these species were contributing to CRISPR-Cas protein

1 production (**Supp. Table 12**). These data also show that Thieb-B clade members are present and active
2 in the Atlantic Ocean.

3 Research shows that CRISPR-Cas adaptation (*i.e.*, protospacer incorporation into spacer arrays)
4 requires Cas1 or Cas2 to respond to new MGE threats (19, 67). Thus the absence of these proteins in
5 our metaproteome could suggest that the *T. thiebautii* CRISPR-Cas system is not actively adapting to
6 new phage and is perhaps performing alternative functions in the cell independent of viral immunity (84,
7 85). Three observations argue against this supposition. **1.** Self-targeting spacers (*i.e.*, matching
8 alternative sites in the MAG) were not identified, suggesting that interference-based gene regulation is not
9 occurring (e.g., (84–86)). **2.** Most of the spacers detected in each MAG are distinct from those in other
10 MAGs, suggesting that ‘rapid’ adaptation occurs in *T. thiebautii* (69, 87), **3.** Read recruiting from Pacific
11 Ocean *Trichodesmium* community data collected by others (88) shows that all annotated *T. thiebautii* H94
12 cas genes are expressed (including *cas1* and *cas2*), and they appear to have diel periodicity (**Supp. Fig.**
13 **2**). Thus, while we cannot exclude alternative CRISPR functions in *T. thiebautii*, our data strongly suggest
14 CRISPR-Cas mediated phage immunity is commonplace in the clade.

15

16 **Conclusions**

17 Herein we show that all N₂-fixing *Trichodesmium* genomes are large, low protein-coding, and
18 repeat-rich, with *T. thiebautii* having increased singleton gene clusters. Additionally, the conserved
19 maintenance of a functional CRISPR-Cas system in *T. thiebautii* is a defining speciation difference
20 between the major clades of *Trichodesmium* and is likely an important factor in their numerical dominance
21 over *T. erythraeum*. Our findings also raise questions about future oceanic N₂ fixation – will *T. erythraeum*
22 be a climate change winner as predicted (14, 20) or will increased phage infectivity reduce their future
23 expansion?

24 The combination of singleton gene enrichment and conserved CRISPR-Cas systems in *T.*
25 *thiebautii* suggests that immunity allows the recipients of transduced genes to survive and thereby
26 increase their genetic diversity (as noted elsewhere in other systems (89, 90)). Interestingly, CRISPRs
27 are relatively rare in marine systems, and fittingly the numerically dominant planktonic bacteria (e.g.,

1 *Prochlorococcus*, *Synechococcus*, and *Pelagibacter*) do not have CRISPR-Cas systems. Furthermore,
2 many well-described CRISPR-Cas systems are biogeographically confined (*i.e.*, hot springs) or human
3 health-related. Because of these issues, we are only just beginning to address how MGE selection
4 maintains CRISPR-Cas systems in global populations (81). Thus, *Trichodesmium* colonies represent a
5 globally distributed ‘ecosystem’ to further study MGE-CRISPR-Cas function in a biogeochemically crucial
6 context.

7

8 Materials and Methods

9 **Trichodesmium colony collection.** *Trichodesmium* colonies were collected with a hand-towed (~150 ft
10 of line) 130- μ m Sea Gear plankton net on February 8th thru March 11th, 2018, during the R/V Atlantis
11 TriCoLim cruise (AT39-05) that transected from the Cape Verde Islands to Puerto Rico (**Fig. 1**). Colonies
12 were rapidly removed from the cod end and picked separately into tuft and puff morphologies with sterile
13 plastic disposable Pasteur pipettes into sterilized seawater 50 ml Falcon tubes. These morphology-
14 segregated samples were sequentially washed two times, gently filtered down onto 5- μ m polycarbonate
15 membranes, and rapidly frozen in liquid N₂ until processing back at the laboratory.

16 **DNA Isolation and Sequencing.** High-quality DNA was isolated from ~50 frozen colonies per station via
17 Qiagen DNeasy Powersoil Kit (Germantown, MD) using the manufacturer’s protocol with the following
18 exceptions. Frozen colony samples were rapidly transferred to bead beating tubes with the 5- μ m filter
19 unwrapped around the inside of the tube, rendering the biomass containing surface available to the
20 beads. DNA quality and quantity was determined via NanoDrop UV-Vis spectrophotometer and Qubit
21 Fluorometer, respectively (ThermoFisher; Waltham, MA). Samples with lower [DNA] and/or quality were
22 cleaned up with the Qiagen PowerClean Pro DNA clean up kit (Germantown, MD). DNA from twelve
23 TriCoLim samples were 150 PE Illumina sequenced by Novogene (Sacramento, CA) to a final depth of 25
24 Gbps. DNA was isolated from frozen *T. thiebautii* H94 samples using the same protocol as above and
25 was sequenced via 250PE Illumina MiSeq at the USC Epigenome Center (1.8 Gbps total) because the
26 original assembly in (21) was poor quality. Raw reads are available at NCBI’s SRA under the BioProject
27 PRJNA828267.

1 **Isolate and Field MAG Assembly.** Both the field samples and *T. thiebautii* H94 reads were run through
2 similar assembly pipelines, but the latter was assembled on KBase (<https://www.kbase.us>), while the
3 former were on a Linux server. The quality of reads was checked with FastQC v0.11.2 (91) and trimmed
4 to enhance stats using Trimmomatic v0.33 (92). MAGs were assembled de novo using metaSPAdes
5 v3.12.0 (93) for H94 and MEGAHIT v1.2.6 (94) for the TriCoLim samples. Binning of contigs was
6 performed via MaxBin2 v2.2.4, quality was checked with CheckM v1.1.3 (22), and phylogenetic
7 placement of the MAGs was determined with GTDB-tk v1.3.0 (95). Field MAGs were dereplicated using
8 fastANI (96) with a cutoff of 98.5% ID. Dereplicated bins >50% CheckM complete were hand refined in
9 Anvi'o v7 (28, 29) until contamination level was below 5%. *T. erythraeum* strain 2175 was downloaded
10 from NCBI and was hand-refined in Anvi'o (28, 29) to remove contaminating contigs using the TriCoLim
11 reads, and its final genome stats were determined with CheckM (22).

12 **Phylogenomics.** Higher quality *Trichodesmium* MAGs (>50% complete; **Supp. Table 1**) and nearest
13 relative genomes downloaded from the NCBI Assembly page were run through the program GToTree
14 v1.6.12 to define a initial guide tree based on 251 cyanobacterial core protein Hidden Markov Models (97,
15 98). Alignment and partition files from GToTree were piped to IQtree v2.1.4-beta in ModelFinder
16 optimality mode with 1000 ultrafast bootstraps to generate the phylogenomic tree (99). The tree was
17 visualized and edited in the interactive Tree of Life (iTol; (100)).

18 **Metapangenomics.** The metapangenomic pipeline in Anvi'o was used to characterize shared and distinct
19 gene clusters (GCs) in the MAGs and determine if these GCs were represented in the TriCoLim reads
20 (28, 29). Briefly, this pipeline creates a contig database for all MAGs that was then annotated with
21 prodigal (31), COGs (32), PFAMS (33), KOFAM (50) and KEGG (51). Reads were recruited to contigs in
22 the Anvi'o database with TriCoLim read samples using bowtie2 v 2.4.1 (101), matching Sequence
23 Alignment/Map (SAMs) were converted to binary alignment maps (BAMs) with SAMtools v1.11 (102), and
24 BAMs were profiled across the TriCoLim read sets using Anvi'o to determine environmental auxiliary and
25 environmental core genes (EAG and ECG, respectively). COG categories per 100kb was determined by
26 exporting the annotation from Anvi'o, determining the COG categories per MAG, summing those results
27 per clade, and then analyzing and graphing in R v 4.0.3 (2020-10-10) with R Studio v1.4.1103 (103).
28 Differences between COG category counts per clades were tested for statistical significance using

1 ANOVA in the R package rstatix (104). The same general pipeline was used to determine single gene
2 copy per clade and toxin:antitoxin GCs per clade. The Anvio summary data was converted into a matrix
3 via the scripts in (105) and used with the R package micropan (56) to generate Heaps' law alpha value
4 and genome fluidity estimates.

5 **CRISPR-Cas Analyses.** CRISPRCasTyper (59) was used for the annotation of CRISPR-Cas systems'
6 subtypes, associated *cas* genes, and CRISPR arrays for all genome assemblies of *Trichodesmium spp.*
7 and MAGs from their nearest relatives (*i.e.*, *Okeania* sp. SIO2F4, *Okeania* sp. SIO3I5, and *Hydrocoleum*
8 sp. CS-963). The raw output from this program identified CRISPR-Cas systems in multiple contigs in each
9 draft genome and is shown in a phylogenomic context in **Fig. 4A**. Because many of the MAGs were
10 fragmented, CRISPR-Cas system portions on other contigs are shown with double slashes if (1) the
11 pieces were found on the edges of their located contigs, and (2) the associated *cas* genes are still
12 predicted to be part of the subtype III-B, I-D, or III-D systems defined in (19). Additional annotations for
13 accessory genes (purple) and hypothetical genes (grey) were determined by CRISPRCasTyper,
14 CRISPRCasFinder, and BLAST (30, 59, 106, 107).

15 We used clustal in the program Geneious Prime (Biomatters, San Diego, CA) to align Cas10
16 protein sequences from all genomes in **Fig. 4A**, and RaxML v8 to generate the maximum likelihood
17 phylogenetic tree with 100 bootstraps (108).

18 **Virome Assembly.** We screened for putative phage genome, prophage or plasmid fragments in
19 TriCoLim and enrichment culture assemblies using the virsorter2, DRAM-V, and checkV pipelines for
20 viruses and metaplasmidSPAdes for plasmids (75–77, 109). The contig sequences supplied from these
21 efforts were used to generate custom blast databases (107) that were subsequently screened with
22 *Trichodesmium* spacers defined above. No hits were defined in the plasmid database, while many high-
23 quality spacer hits were found with DRAM-V putative phage sequences (**Supp. Table 8**). We used
24 FastANI on contigs matching *Trichodesmium* spacers to group them based on >98.1% identity and show
25 that very similar sequences assembled from independent stations (**Supp. Table 9**).

26 **Proteome analysis of *Trichodesmium* enriched field samples.** The raw proteome spectra for this
27 manuscript were collected for a prior work (83) and newly analyzed for this study. Briefly, proteome

1 samples were acquired by gentle hand picking from the phytoplankton nets, rinsed thrice in 0.2- μ m
2 filtered trace-metal-clean surface seawater and then decanted onto 0.2- μ m supor filters and immediately
3 frozen at -80°C until protein extraction. Proteins were extracted using a detergent based method and
4 digested while embedded in a polyacrylamide gel, as previously described (83, 110, 111). The global
5 metaproteomes were analyzed by online nanoflow two-dimension active modulation reversed phase-
6 reversed phase liquid chromatography mass spectrometry using a Thermo Orbitrap Fusion instrument
7 (83, 112).

8 Raw spectra were searched with the Sequest algorithm implemented in Proteome Discoverer 2.2
9 using a custom-built genomic database consisting of the pan genome of *Trichodesmium*, plus
10 *Trichodesmium* MAGs reported in this study. To avoid inflation of the sequence database and later
11 misinterpretation of phylogenetic signals, only one version of any identical/redundant protein sequences
12 were included in the database, with the possible phylogenetic attributions for the redundant proteins
13 noted in downstream phylogenetic analyses. Sequest mass tolerances were set to +/- 10ppm (parent)
14 and +/- 0.6 Dalton (fragment). Fixed Cysteine modification of +57.022, and variable N-terminal acetylation
15 of + 42 and methionine modification of +16 were included. Protein identifications were made with Peptide
16 Prophet in Scaffold (Proteome Software) at the 80% peptide threshold minimum, resulting in an estimated
17 peptide FDR of 1.5% and an estimated protein FDR of 0.0%. Relative protein abundances are reported
18 as normalized total exclusive spectral counts, so only spectra corresponding to a specific peptide for a
19 given protein were considered. This avoids the problem of overlapping peptides in the phylogenetic
20 analysis. The values are normalized to total spectral counts identified in each sample. The general
21 workflow for assigning phylogenetic specificity was as follows: if an identified protein was already a
22 member of the *Trichodesmium* core genome, the core designation was retained; for remaining proteins, if
23 all peptide evidence for that protein was present in both *T. erythraeum* and *T. thiebautii* MAGs, the protein
24 was also considered to be "core." Otherwise, the peptide was assigned to its corresponding MAG
25 phylogeny. Thus, only peptides specific to a given *Trichodesmium* species was considered for that
26 species. The peptides identified for the CRISPR-Cas proteins were further checked using the Metatryp
27 2.0 tool (www.metatryp.whoi.edu) (113) to ensure phylogenetic specificity of the signals, i.e. to the *T.*
28 *thiebautii* MAGS specifically mentioned in the text.

1 The mass spectrometry proteomics data were originally deposited in the ProteomeXchange
2 Consortium via the PRIDE partner repository with the identifier PXD016225 and can be accessed
3 at <https://doi.org/10.6019/PXD016225> (114, 115). The data is also available at BCO-DMO
4 (<https://www.bco-dmo.org/dataset/787078>). The newly searched protein identifications are furthermore
5 provided as **Supp. Tables 10-12**.

6 **Transcriptome read recruiting.** *Trichodesmium* colony metatranscriptomes were downloaded from
7 NCBI SRA (projects PRJNA381915 and PRJNA374879) and mapped against all cas genes from H94 and
8 cas10 from MAG *T. thiebautii* Indian Ocean that is a representative of cluster 3 in **Fig. 4B**. Read quality
9 was checked with FastQC v0.11.2 (91), trimmed with Trimmomatic v0.33 (92), recruited to cas genes with
10 Bowtie v 2.4.1, converted to BAMs with Samtools v1.11, and profiled in Anvi'o v7.0. Average read depth
11 values were normalized with the constitutive *Trichodesmium* gene *rotA*, as in (116). Gene targets and
12 results are summarized in **Supp. Tables 13-15**, and the data were visualized in R v 4.0.3 (2020-10-10)
13 with R Studio v1.4.1103 (103) and shown in **Supp. Fig 2**.

14
15 **Acknowledgments**
16

17 We would like to thank the captain and crew of the RV Atlantis for their essential role in sample collection
18 and providing a safe and efficient platform for marine microbiology. This work was funded by NSF grants
19 OCE 1657757 and OCE 1851222 to DAH, FXF, and EAW, OCE 1850719 to MAS, and by discretionary
20 USC funds to EAW.

1 **References Cited**

2 1. C. M. Moore, *et al.*, Processes and patterns of oceanic nutrient limitation. *Nat Geosci* **6**,
3 701–710 (2013).

4 2. J. A. Sohm, E. A. Webb, D. G. Capone, Emerging patterns of marine nitrogen fixation. *Nat*
5 *Rev Microbiol* **9**, 499–508 (2011).

6 3. J. P. Zehr, D. G. Capone, Changing perspectives in marine nitrogen fixation. *Science* **368**
7 (2020).

8 4. C. Wu, *et al.*, Evidence of the Significant Contribution of Heterotrophic Diazotrophs to
9 Nitrogen Fixation in the Eastern Indian Ocean During Pre-Southwest Monsoon Period.
10 *Ecosystems* (2021) <https://doi.org/10.1007/s10021-021-00702-z> (October 12, 2021).

11 5. T. O. Delmont, Discovery of nondiazotrophic *Trichodesmium* species abundant and
12 widespread in the open ocean. *Proc Natl Acad Sci USA* **118**, e2112355118 (2021).

13 6. D. Capone, J. Zehr, H. Paerl, B. Bergman, E. Carpenter, *Trichodesmium*, a Globally Significant
14 Marine Cyanobacterium. *Science* **276**, 1221 (1997).

15 7. A. M. Hynes, E. A. Webb, S. C. Doney, J. B. Waterbury, Comparison of Cultured
16 *Trichodesmium* (Cyanophyceae) with Species Characterized from the Field. *J Phycol* **48**,
17 196–210 (2012).

18 8. E. A. Webb, R. Foster, T. A. Villareal, J. B. Waterbury, J. Zehr, “Genus *Trichodesmium*” in
19 *Bergey’s Manual of Systematics of Archaea and Bacteria*, in press., (2022).

20 9. M. Rouco, H. J. Warren, D. J. McGillicuddy, J. B. Waterbury, S. T. Dyhrman, *Trichodesmium*
21 sp. clade distributions in the western North Atlantic Ocean. *Limnol Oceanogr* **59**, 1899–
22 1909 (2014).

23 10. D. G. Capone, *et al.*, Nitrogen fixation by *Trichodesmium* spp.: An important source of new
24 nitrogen to the tropical and subtropical North Atlantic Ocean. *Global Biogeochem Cy* **19**
25 (2005).

26 11. D. Karl, *et al.*, The role of nitrogen fixation in biogeochemical cycling in the subtropical
27 North Pacific Ocean. *Nature* **388**, 533–538 (1997).

28 12. S. Janson, B. Bergman, E. Carpenter, S. Giovannoni, K. Vergin, Genetic analysis of natural
29 populations of the marine diazotrophic cyanobacterium *Trichodesmium*. *FEMS*
30 *Microbiology Ecology* **30**, 57 65 (1999).

31 13. E. J. Carpenter, *et al.*, The tropical diazotrophic phytoplankton *Trichodesmium*:biological
32 characteristics of two common species. *Mar Ecol Prog Ser* **95**, 295–304 (1993).

1 14. D. A. Hutchins, F.-X. Fu, E. A. Webb, N. Walworth, A. Tagliabue, Taxon-specific response of
2 marine nitrogen fixers to elevated carbon dioxide concentrations. *Nat Geosci* **6**, 790–795
3 (2013).

4 15. P. D. Chappell, E. A. Webb, A molecular assessment of the iron stress response in the two
5 phylogenetic clades of *Trichodesmium*. *Environ Microbiol* **12**, 13–27 (2010).

6 16. P. Lundgren, E. Soderback, A. Singer, E. Carpenter, B. Bergman, *Katagnymene*:
7 Characterization of a novel marine diazotroph. *Journal Of Phycology* **37**, 1052–1062
8 (2001).

9 17. M. Rouco, *et al.*, Variable depth distribution of *Trichodesmium* clades in the North Pacific
10 Ocean. *Env Microbiol Rep* **8**, 1058–1066 (2016).

11 18. P. D. Chappell, J. W. Moffett, A. M. Hynes, E. A. Webb, Molecular evidence of iron limitation
12 and availability in the global diazotroph *Trichodesmium*. *ISMEJ* **6**, 1728–1739 (2012).

13 19. K. S. Makarova, *et al.*, Evolutionary classification of CRISPR–Cas systems: a burst of class 2
14 and derived variants. *Nature Reviews Microbiology* **18**, 67–83 (2020).

15 20. M. R. Gradoville, A. E. White, D. Böttjer, M. J. Church, R. M. Letelier, Diversity trumps
16 acidification: Lack of evidence for carbon dioxide enhancement of *Trichodesmium*
17 community nitrogen or carbon fixation at Station ALOHA. *Limnol Oceanogr* **59** (2014).

18 21. N. Walworth, *et al.*, *Trichodesmium* genome maintains abundant, widespread noncoding
19 DNA in situ, despite oligotrophic lifestyle. *Proc National Acad Sci* **112**, 4251–4256 (2015).

20 22. D. H. Parks, M. Imelfort, C. T. Skennerton, P. Hugenholtz, G. W. Tyson, CheckM: assessing
21 the quality of microbial genomes recovered from isolates, single cells, and metagenomes.
22 *Genome Res* **25**, 1043–1055 (2015).

23 23. S. J. Giovannoni, J. C. Thrash, B. Temperton, Implications of streamlining theory for
24 microbial ecology. *ISMEJ* **8**, 1553–1565 (2014).

25 24. K. M. Orcutt, *et al.*, Characterization of *Trichodesmium* spp. by genetic techniques. *Applied
26 And Environmental Microbiology* **68**, 2236–2245 (2002).

27 25. G. Rocap, D. L. Distel, J. B. Waterbury, S. W. Chisholm, Resolution of *Prochlorococcus* and
28 *Synechococcus* ecotypes by using 16S-23S ribosomal DNA internal transcribed spacer
29 sequences. *Appl Environ Microb* **68**, 1180–1191 (2002).

30 26. J. A. Sohm, *et al.*, Co-occurring *Synechococcus* ecotypes occupy four major oceanic regimes
31 defined by temperature, macronutrients and iron. *ISMEJ* **10**, 333 EP-345 (2016).

32 27. N. Kashtan, *et al.*, Single-Cell Genomics Reveals Hundreds of Coexisting Subpopulations in
33 Wild *Prochlorococcus*. *Science* **344**, 416–420 (2014).

- 1 28. A. M. Eren, *et al.*, Anvi'o: an advanced analysis and visualization platform for 'omics data.
- 2 *Peerj* **3**, e1319 (2015).
- 3 29. A. M. Eren, *et al.*, Community-led, integrated, reproducible multi-omics with anvi'o. *Nature Microbiology* **6**, 3–6 (2021).
- 4
- 5 30. S. F. Altschul, W. Gish, W. Miller, E. W. Myers, D. J. Lipman, Basic local alignment search
- 6 tool. *Journal of Molecular Biology* **215**, 403–410 (1990).
- 7 31. D. Hyatt, *et al.*, Prodigal: prokaryotic gene recognition and translation initiation site
- 8 identification. *Bmc Bioinformatics* **11**, 119 (2010).
- 9 32. M. Y. Galperin, *et al.*, COG database update: focus on microbial diversity, model organisms,
- 10 and widespread pathogens. *Nucleic Acids Research* **49**, D274–D281 (2021).
- 11 33. J. Mistry, *et al.*, Pfam: The protein families database in 2021. *Nucleic Acids Research* **49**,
- 12 D412–D419 (2021).
- 13 34. N. Toro, F. Martínez-Abarca, M. D. Molina-Sánchez, F. M. García-Rodríguez, R. Nisa-
- 14 Martínez, Contribution of Mobile Group II Introns to *Sinorhizobium meliloti* Genome
- 15 Evolution. *Frontiers in Microbiology* **9** (2018).
- 16 35. X. Dong, G. Qu, C. L. Piazza, M. Belfort, Group II intron as cold sensor for self-preservation
- 17 and bacterial conjugation. *Nucleic Acids Research* **48**, 6198–6209 (2020).
- 18 36. A. M. Pyle, Group II Intron Self-Splicing. *Annual Review of Biophysics* **45**, 183–205 (2016).
- 19 37. U. Pfreundt, W. R. Hess, Sequential splicing of a group II twintron in the marine
- 20 cyanobacterium *Trichodesmium*. *Sci Rep-uk* **5**, 16829 (2015).
- 21 38. M. A. Brockhurst, *et al.*, The Ecology and Evolution of Pangenomes. *Current Biology* **29**,
- 22 R1094–R1103 (2019).
- 23 39. N. V. Fedoroff, Transposable Elements, Epigenetics, and Genome Evolution. *Science* **338**,
- 24 758–767 (2012).
- 25 40. K. Blin, *et al.*, antiSMASH 6.0: improving cluster detection and comparison capabilities.
- 26 *Nucleic Acids Research* **49**, W29–W35 (2021).
- 27 41. Z. Chang, *et al.*, Biosynthetic pathway and gene cluster analysis of curacin A, an antitubulin
- 28 natural product from the tropical marine cyanobacterium *Lyngbya majuscula*. *J Nat Prod*
- 29 **67**, 1356–1367 (2004).
- 30 42. R. C. Coates, *et al.*, Characterization of cyanobacterial hydrocarbon composition and
- 31 distribution of biosynthetic pathways. *PLoS One* **9**, e85140 (2014).

1 43. S. Basu, Y. Shaked, Mineral iron utilization by natural and cultured *Trichodesmium* and
2 associated bacteria. *Limnol Oceanogr* **63**, 2307–2320 (2018).

3 44. S. Basu, M. Gledhill, D. de Beer, S. G. P. Matondkar, Y. Shaked, Colonies of marine
4 cyanobacteria *Trichodesmium* interact with associated bacteria to acquire iron from dust.
5 *Commun Biology* **2**, 1–8 (2019).

6 45. K. S. Makarova, N. V. Grishin, E. V. Koonin, The HicAB cassette, a putative novel, RNA-
7 targeting toxin-antitoxin system in archaea and bacteria. *Bioinformatics* **22**, 2581–2584
8 (2006).

9 46. A. Fiebig, C. M. Castro Rojas, D. Siegal-Gaskins, S. Crosson, Interaction specificity, toxicity
10 and regulation of a paralogous set of ParE/RelE-family toxin–antitoxin systems. *Molecular
11 Microbiology* **77**, 236–251 (2010).

12 47. A. Sharrock, A. Ruthe, E. S. V. Andrews, V. A. Arcus, J. L. Hicks, VapC proteins from
13 *Mycobacterium tuberculosis* share ribonuclease sequence specificity but differ in
14 regulation and toxicity. *PLOS ONE* **13**, e0203412 (2018).

15 48. S. Doron, *et al.*, Systematic discovery of antiphage defense systems in the microbial
16 pangenome. *Science* **359**, eaar4120- (2018).

17 49. K. S. Makarova, *et al.*, An updated evolutionary classification of CRISPR–Cas systems. *Nature
18 Reviews Microbiology* **13**, 722–736 (2015).

19 50. T. Aramaki, *et al.*, KofamKOALA: KEGG Ortholog assignment based on profile HMM and
20 adaptive score threshold. *Bioinformatics* **36**, 2251–2252 (2020).

21 51. M. Kanehisa, Y. Sato, KEGG Mapper for inferring cellular functions from protein sequences.
22 *Protein Sci* **28**, 27 (2019).

23 52. A. O. Kislyuk, B. Haegeman, N. H. Bergman, J. S. Weitz, Genomic fluidity: an integrative view
24 of gene diversity within microbial populations. *BMC Genomics* **12**, 32 (2011).

25 53. E. J. Carpenter, A. Subramaniam, D. Capone, Biomass and primary productivity of the
26 cyanobacterium *Trichodesmium* spp. in the tropical N Atlantic Ocean. *Deep Sea Res Part
27 Oceanogr Res Pap* **51**, 173–203 (2004).

28 54. Y. W. Luo, *et al.*, Database of diazotrophs in global ocean: abundance, biomass and nitrogen
29 fixation rates. *Earth Syst Sci Data* **4**, 47–73 (2012).

30 55. J. T. Evans, V. J. Denef, To Dereplicate or Not To Dereplicate? *mSphere* (2020)
31 <https://doi.org/10.1128/mSphere.00971-19> (February 20, 2022).

32 56. L. Snipen, K. H. Liland, micropan: an R-package for microbial pan-genomics. *BMC
33 Bioinformatics* **16**, 79 (2015).

1 57. H. Tettelin, D. Riley, C. Cattuto, D. Medini, Comparative genomics: the bacterial pan-
2 genome. *Current Opinion in Microbiology* **11**, 472–477 (2008).

3 58. N. A. Andreani, E. Hesse, M. Vos, Prokaryote genome fluidity is dependent on effective
4 population size. *ISMEJ* **11**, 1719–1721 (2017).

5 59. J. Russel, R. Pinilla-Redondo, D. Mayo-Muñoz, S. A. Shah, S. J. Sørensen, CRISPRCasTyper:
6 Automated Identification, Annotation, and Classification of CRISPR-Cas Loci. *The CRISPR
7 Journal* **3**, 462–469 (2020).

8 60. E. R. Westra, A. J. Dowling, J. M. Broniewski, S. van Houte, Evolution and Ecology of CRISPR.
9 *Annual Review of Ecology, Evolution, and Systematics* **47**, 307–331 (2016).

10 61. D. Burstein, *et al.*, Major bacterial lineages are essentially devoid of CRISPR-Cas viral
11 defence systems. *Nat Commun* **7**, 10613 (2016).

12 62. D. Burstein, *et al.*, New CRISPR–Cas systems from uncultivated microbes. *Nature* **542**, 237–
13 241 (2017).

14 63. A. Bernheim, R. Sorek, The pan-immune system of bacteria: antiviral defence as a
15 community resource. *Nature Reviews Microbiology* **18**, 113–119 (2020).

16 64. L. A. Marraffini, CRISPR-Cas immunity in prokaryotes. *Nature* **526**, 55–61 (2015).

17 65. S. Silas, *et al.*, Type III CRISPR-Cas systems can provide redundancy to counteract viral
18 escape from type I systems. *eLife* **6** (2017).

19 66. M. V. Kolesnik, I. Fedorova, K. A. Karneyeva, D. N. Artamonova, K. V. Severinov, Type III
20 CRISPR-Cas Systems: Deciphering the Most Complex Prokaryotic Immune System.
21 *Biochemistry Moscow* **86**, 1301–1314 (2021).

22 67. D. Artamonova, *et al.*, Spacer acquisition by Type III CRISPR–Cas system during
23 bacteriophage infection of *Thermus thermophilus*. *Nucleic Acids Research* **48**, 9787–9803
24 (2020).

25 68. M. A. Estrella, F.-T. Kuo, S. Bailey, RNA-activated DNA cleavage by the Type III-B CRISPR–Cas
26 effector complex. *Genes & Development* **30**, 460–470 (2016).

27 69. A. F. Andersson, J. F. Banfield, Virus Population Dynamics and Acquired Virus Resistance in
28 Natural Microbial Communities. *Science* **320**, 1047–50 (2008).

29 70. V. A. Sorokin, M. S. Gelfand, I. I. Artamonova, Evolutionary Dynamics of Clustered Irregularly
30 Interspaced Short Palindromic Repeat Systems in the Ocean Metagenome. *Appl. Environ.
31 Microbiol.* **76**, 2136–2144 (2010).

1 71. M. E. Berg Miller, *et al.*, Phage–bacteria relationships and CRISPR elements revealed by a
2 metagenomic survey of the rumen microbiome. *Environmental Microbiology* **14**, 207–227
3 (2012).

4 72. J. B. Emerson, *et al.*, Virus-Host and CRISPR Dynamics in Archaea-Dominated Hypersaline
5 Lake Tyrrell, Victoria, Australia. *Archaea* **2013**, e370871 (2013).

6 73. S. Roux, *et al.*, Ecology and evolution of viruses infecting uncultivated SUP05 bacteria as
7 revealed by single-cell- and meta-genomics. *eLife* **3**, e03125 (2014).

8 74. S. Martínez Arbas, *et al.*, Roles of bacteriophages, plasmids and CRISPR immunity in
9 microbial community dynamics revealed using time-series integrated meta-omics. *Nature
10 Microbiology* **6**, 123–135 (2021).

11 75. J. Guo, *et al.*, VirSorter2: a multi-classifier, expert-guided approach to detect diverse DNA
12 and RNA viruses. *Microbiome* **9**, 37 (2021).

13 76. M. Shaffer, *et al.*, DRAM for distilling microbial metabolism to automate the curation of
14 microbiome function. *Nucleic Acids Research* **48**, 8883–8900 (2020).

15 77. D. Antipov, M. Raiko, A. Lapidus, P. A. Pevzner, Plasmid detection and assembly in genomic
16 and metagenomic data sets. *Genome Res* **29**, 961–968 (2019).

17 78. N. C. Pyenson, K. Gayvert, A. Varble, O. Elemento, L. A. Marraffini, Broad Targeting
18 Specificity during Bacterial Type III CRISPR-Cas Immunity Constrains Viral Escape. *Cell Host
19 & Microbe* **22**, 343–353.e3 (2017).

20 79. B. N. J. Watson, J. A. Steens, R. H. J. Staals, E. R. Westra, S. van Houte, Coevolution between
21 bacterial CRISPR-Cas systems and their bacteriophages. *Cell Host & Microbe* **29**, 715–725
22 (2021).

23 80. J. A. Steens, *et al.*, SCOPE enables type III CRISPR-Cas diagnostics using flexible targeting and
24 stringent CARF ribonuclease activation. *Nat Commun* **12**, 5033 (2021).

25 81. E. R. Westra, B. R. Levin, It is unclear how important CRISPR-Cas systems are for protecting
26 natural populations of bacteria against infections by mobile genetic elements. *PNAS* **117**,
27 27777–27785 (2020).

28 82. B. G. Paul, A. M. Eren, Eco-evolutionary significance of domesticated retroelements in
29 microbial genomes. *Mobile DNA* **13**, 6 (2022).

30 83. N. A. Held, *et al.*, Co-occurrence of Fe and P stress in natural populations of the marine
31 diazotroph *Trichodesmium*. *Biogeosciences* **17**, 2537–2551 (2020).

1 84. H. K. Ratner, T. R. Sampson, D. S. Weiss, I can see CRISPR now, even when phage are gone: a
2 view on alternative CRISPR-Cas functions from the prokaryotic envelope. *Curr Opin Infect*
3 *Dis* **28**, 267–274 (2015).

4 85. E. R. Westra, A. Buckling, P. C. Fineran, CRISPR–Cas systems: beyond adaptive immunity.
5 *Nature Reviews Microbiology* **12**, 317–326 (2014).

6 86. F. Wimmer, C. L. Beisel, CRISPR-Cas Systems and the Paradox of Self-Targeting Spacers.
7 *Front. Microbiol.* **10** (2020).

8 87. G. W. Tyson, J. F. Banfield, Rapidly evolving CRISPRs implicated in acquired resistance of
9 microorganisms to viruses. *Environmental Microbiology* **10**, 200–207 (2008).

10 88. K. R. Frischkorn, S. T. Haley, S. T. Dyhrman, Coordinated gene expression between
11 *Trichodesmium* and its microbiome over day–night cycles in the North Pacific Subtropical
12 Gyre. *ISMEJ* **37**, 1 (2018).

13 89. B. N. J. Watson, R. H. J. Staals, P. C. Fineran, CRISPR-Cas-Mediated Phage Resistance
14 Enhances Horizontal Gene Transfer by Transduction. *mBio* **9** (2018).

15 90. A. Varble, S. Meaden, R. Barrangou, E. R. Westra, L. A. Marraffini, Recombination between
16 phages and CRISPR–cas loci facilitates horizontal gene transfer in *Staphylococci*. *Nat*
17 *Microbiol* **4**, 956–963 (2019).

18 91. , Babraham Bioinformatics - FastQC A Quality Control tool for High Throughput Sequence
19 Data (September 11, 2020).

20 92. A. M. Bolger, M. Lohse, B. Usadel, Trimmomatic: a flexible trimmer for Illumina sequence
21 data. *Bioinformatics* **30**, 2114–2120 (2014).

22 93. S. Nurk, D. Meleshko, A. Korobeynikov, P. A. Pevzner, metaSPAdes: a new versatile
23 metagenomic assembler. *Genome Res.* **27**, 824–834 (2017).

24 94. D. Li, C.-M. Liu, R. Luo, K. Sadakane, T.-W. Lam, MEGAHIT: an ultra-fast single-node solution
25 for large and complex metagenomics assembly via succinct de Bruijn graph. *Bioinformatics*
26 **31**, 1674–1676 (2015).

27 95. P.-A. Chaumeil, A. J. Mussig, P. Hugenholtz, D. H. Parks, GTDB-Tk: a toolkit to classify
28 genomes with the Genome Taxonomy Database. *Bioinformatics* **36**, 1925–1927 (2020).

29 96. C. Jain, L. M. Rodriguez-R, A. M. Phillippy, K. T. Konstantinidis, S. Aluru, High throughput ANI
30 analysis of 90K prokaryotic genomes reveals clear species boundaries. *Nat Commun* **9**,
31 7200 (2018).

32 97. M. D. Lee, GToTree: a user-friendly workflow for phylogenomics. *Bioinformatics* **35**, 4162–
33 4164 (2019).

1 98. M. N. Price, P. S. Dehal, A. P. Arkin, FastTree 2 – Approximately Maximum-Likelihood Trees
2 for Large Alignments. *PLOS ONE* **5**, e9490 (2010).

3 99. B. Q. Minh, *et al.*, IQ-TREE 2: New Models and Efficient Methods for Phylogenetic Inference
4 in the Genomic Era. *Mol Biol Evol* **37**, 1530–1534 (2020).

5 100. I. Letunic, P. Bork, Interactive Tree of Life (iTOL) v5: an online tool for phylogenetic tree
6 display and annotation. *Nucleic Acids Research* **49**, W293–W296 (2021).

7 101. B. Langmead, S. L. Salzberg, Fast gapped-read alignment with Bowtie 2. *Nat Methods* **9**,
8 357–359 (2012).

9 102. P. Danecek, *et al.*, Twelve years of SAMtools and BCFtools. *GigaScience* **10**, giab008 (2021).

10 103. R Core Team, R: A language and environment for statistical computing. R Foundation for
11 Statistical Computing. *R: A language and environment for statistical computing. R*
12 *Foundation for Statistical Computing* (2020) (April 1, 2022).

13 104. A. Kassambara, rstatix: Pipe-friendly framework for basic statistical tests. *R package*
14 *version 0.6. 0* (2020).

15 105. A. Moulana, R. E. Anderson, C. S. Fortunato, J. A. Huber, Selection Is a Significant Driver of
16 Gene Gain and Loss in the Pangenome of the Bacterial Genus *Sulfurovum* in
17 Geographically Distinct Deep-Sea Hydrothermal Vents. *MSystems; Washington* **5** (2020).

18 106. D. Couvin, *et al.*, CRISPRCasFinder, an update of CRISRFinder, includes a portable version,
19 enhanced performance and integrates search for Cas proteins. *Nucleic Acids Research* **46**,
20 W246–W251 (2018).

21 107. C. Camacho, *et al.*, BLAST+: architecture and applications. *BMC Bioinformatics* **10**, 421
22 (2009).

23 108. A. Stamatakis, RAxML version 8: a tool for phylogenetic analysis and post-analysis of large
24 phylogenies. *Bioinformatics* **30**, 1312–1313 (2014).

25 109. S. Nayfach, A. P. Camargo, E. Eloe-Fadrosh, S. Roux, N. Kyrpides, CheckV: assessing the
26 quality of metagenome-assembled viral genomes. *bioRxiv*, 2020.05.06.081778 (2020).

27 110. M. A. Saito, *et al.*, Multiple nutrient stresses at intersecting Pacific Ocean biomes detected
28 by protein biomarkers. *Science* **345**, 1173–1177 (2014).

29 111. X. Lu, H. Zhu, Tube-Gel Digestion. *Molecular & Cellular Proteomics* **4**, 1948–1958 (2005).

30 112. M. R. McIlvin, M. A. Saito, Online Nanoflow Two-Dimension Comprehensive Active
31 Modulation Reversed Phase–Reversed Phase Liquid Chromatography High-Resolution

1 Mass Spectrometry for Metaproteomics of Environmental and Microbiome Samples. *J.*
2 *Proteome Res.* **20**, 4589–4597 (2021).

3 113. J. K. Saunders, *et al.*, METATRYP v 2.0: Metaproteomic Least Common Ancestor Analysis
4 for Taxonomic Inference Using Specialized Sequence Assemblies—Standalone Software
5 and Web Servers for Marine Microorganisms and Coronaviruses. *J. Proteome Res.* **19**,
6 4718–4729 (2020).

7 114. Y. Perez-Riverol, *et al.*, The PRIDE database and related tools and resources in 2019:
8 improving support for quantification data. *Nucleic Acids Research* **47**, D442–D450 (2019).

9 115. N. A. Held, M. A. Saito, *Trichodesmium* field metaproteomes (2019).

10 116. E. D. Orchard, E. A. Webb, S. T. Dyhrman, Molecular analysis of the phosphorus starvation
11 response in *Trichodesmium* spp. *Environ Microbiol* **11**, 2400–2411 (2009).

12

13

14

15

16

1 **Figure Legends**

2

3 **Figure 1.** Map of the 2018 Trans-Atlantic TriCoLim Cruise. Color of the station location indicates hand-
4 picked *Trichodesmium* colony morphology, specifically puff (blue), tuft (black), combined (blue and black),
5 not hand-picked (red), no metagenomic data (grey) and metaproteomic data (asterisk).

6

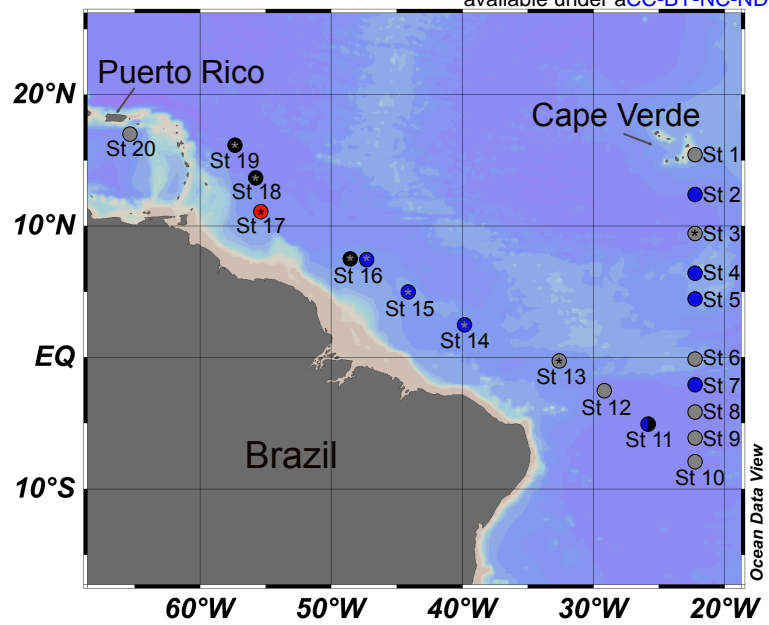
7 **Figure 2.** Phylogenomic tree of *Trichodesmium* and nearest relatives and COG enrichment per 100Kb of
8 *Trichodesmium* clades. In panel **A**, TriCoLim bins are named by station, USCTCC strains are in bold, and
9 names beginning in 'MAG' are from (5). *Trichodesmium* MAGs >80% complete are color coded by clade
10 (i.e., *T. thiebautii* (Blue), *T. erythraeum* A (Black), *T. erythraeum* B (Red), while MAGs <80% are shown in
11 grey. Other *Trichodesmium* MAGs in Supp. Table 1 were excluded from the tree due to low completion
12 values. Panel **B** shows the normalized and summed quantity of COG categories for each MAG per clade.
13 Significantly different categories determined by ANOVA of the mean are denoted above the bracket (p
14 <0.05 =*, <0.01 = **, <0.001 = ***, <0.0001 = ****).
15

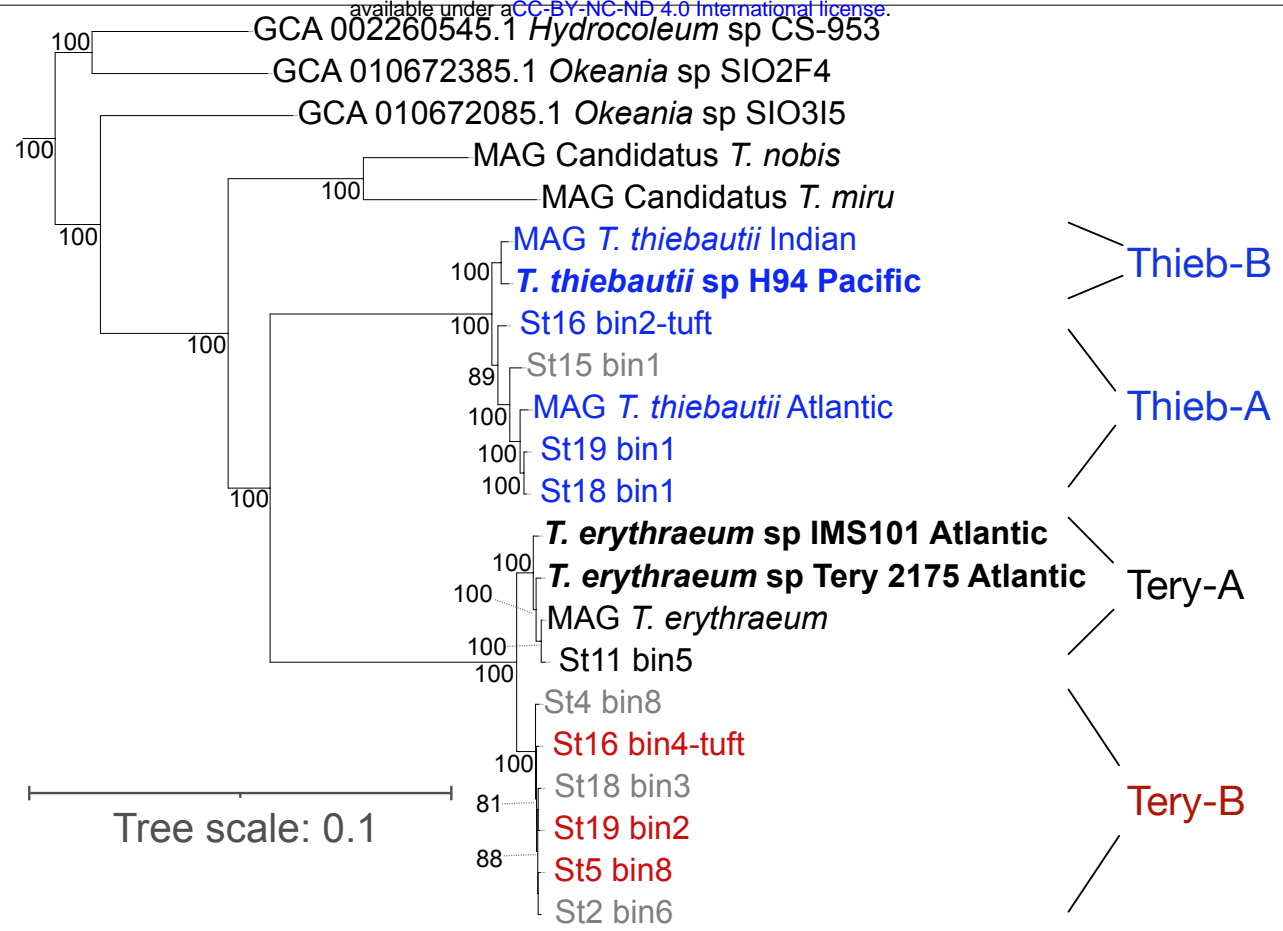
16 **Figure 3.** N₂-fixing *Trichodesmium* Metapangenomic visualization. Panel **A** shows blast-defined
17 conserved gene clusters (GCs) in a MAG as filled colored rings (blue for all *T. thiebautii*, red for *T.*
18 *erythraeum* B, and black for *T. erythraeum* A). Lighter fill colors indicate that those GCs are missing from
19 that MAG. Singleton GCs (i.e., appearing in only one MAG) are mostly shown between 9 and 11 o'clock
20 in the phylogram. The innermost rings of the phylogram indicate number of contributing genomes to a
21 GC, single copy genes (SCG), number of genes in a GC, and max number of paralogs. Continuing
22 outwards, if the GC has annotation it is marked in green, while if it does not it is white. The outermost two
23 rings show whether a GC is environmentally core (green) or auxiliary (red; i.e., the more red the color, the
24 less commonly the GC was observed in TriCoLim reads) and GC homogeneity (i.e., high homogeneity =
25 all green fill). Clear groupings of clade specific auxiliary gene clusters (AGC) are labeled on the edge of
26 the phylogram. Panel **B** shows ANI clustering at the top and the ANI heat map in red. The black heat
27 map shows square root normalized read recruiting to each MAG from TriCoLim (Blacker bars = higher
28 read recruiting). Panel **C** shows statistical analysis of singleton GCs per clade with ANOVA statistical
29 support shown above the brackets (p <0.05 =*, ,0.01 = **).
30

31 **Figure 4.** Presence or absence of CRISPR-Cas genes in a *Trichodesmium* MAGs and their nearest
32 relatives phylogenomic context (**A**) and a maximum likelihood tree of their Cas10 protein sequences (**B**).
33 In **A**, the color-coded, directional shapes on the right represent detected Cas genes (yellow), CRISPR
34 arrays (black), Cas accessory genes (purple) and hypothetical genes (grey) that were annotated by as
35 described in the Materials and Methods. Lighter color indicates lower confidence in the annotation.
36 Double-slashes are contig break positions near the annotated CRISPR-Cas systems, indicating that
37 some clusters are fragmented due to breaks in the assemblies. Gene lengths are not drawn to scale. In
38 **B**, the color coding corresponds to *T. thiebautii* (Blue) and other relatives (Black)
39

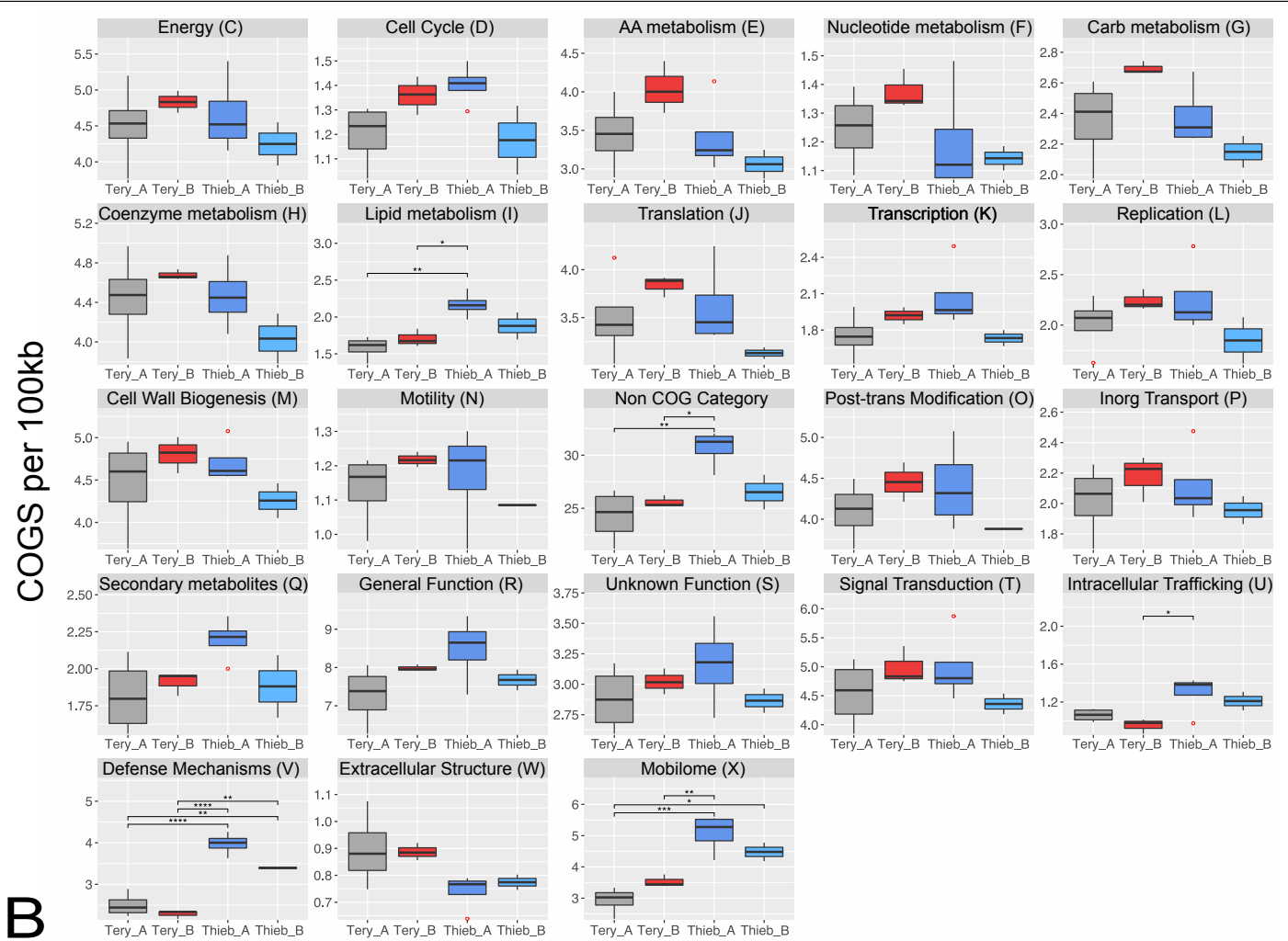
40 **Figure 5.** *Trichodesmium* protein abundances across the TriCoLim transect (**A**) Protein abundance data
41 sorted into *Trichodesmium* phylogenetic groups. Proteins were normalized across each sample, then
42 sorted into the respective phylogenetic group and summed. Error bars indicate the standard deviation of
43 the averaged biological replicates. Quantitation is displayed as normalized spectral counts (see Methods).
44 Core and *T. thiebautii* proteins are much more abundant than those derived from *T. erythraeum*. (**B**)
45 Protein abundance data sorted by biological function. Again, proteins were normalized across each
46 sample, then sorted by COG function and summed. Selected, highly abundant functions are shown. (**C**)
47 Summed normalized protein data for CRISPR-Cas and toxin/antitoxin proteins across the TriCoLim
48 transect. (**D**) Nonsignificant correlation of CRISPR-Cas protein abundances versus *T. thiebautii* total
49 protein abundance (p = 0.88).
50

51

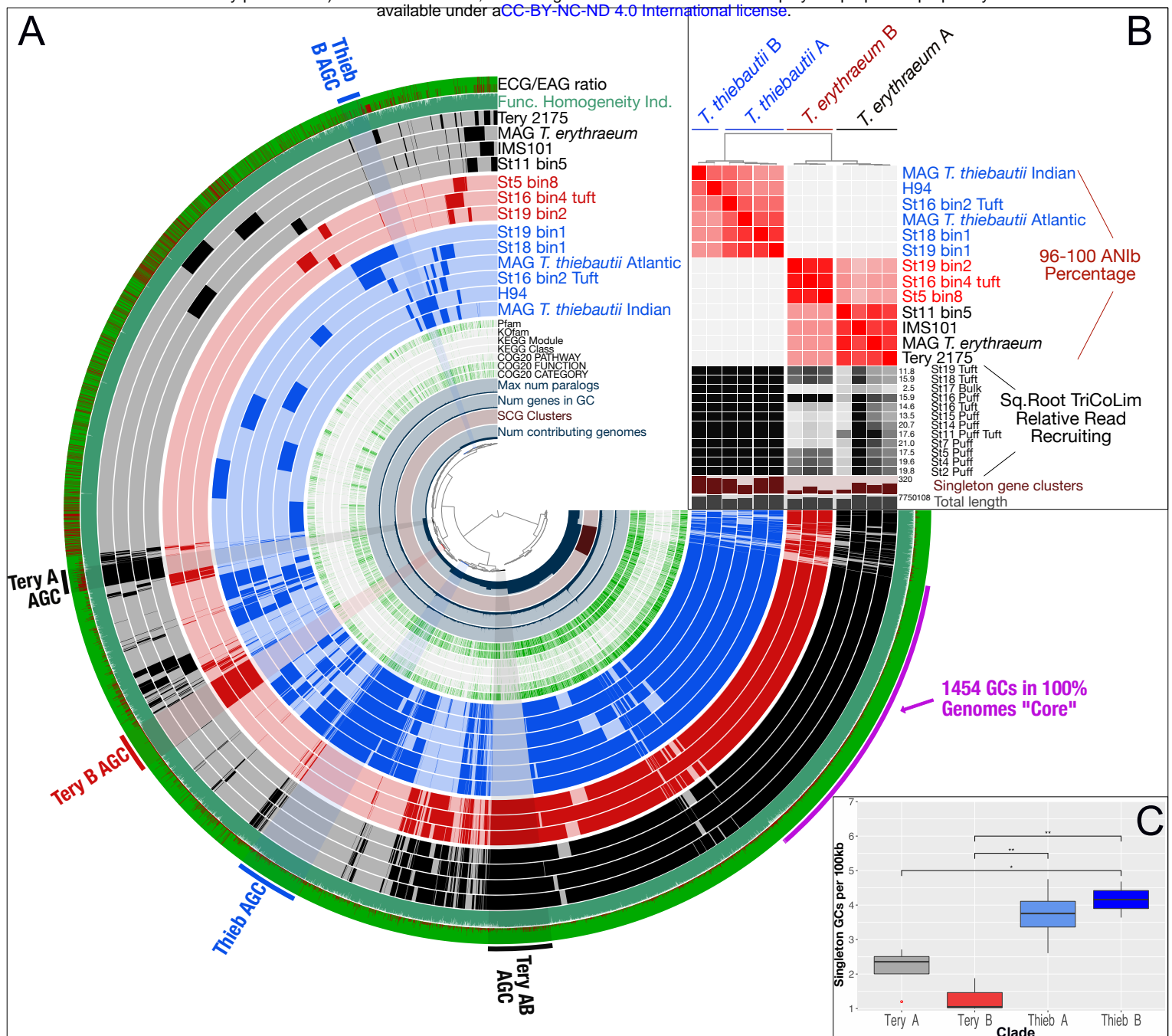


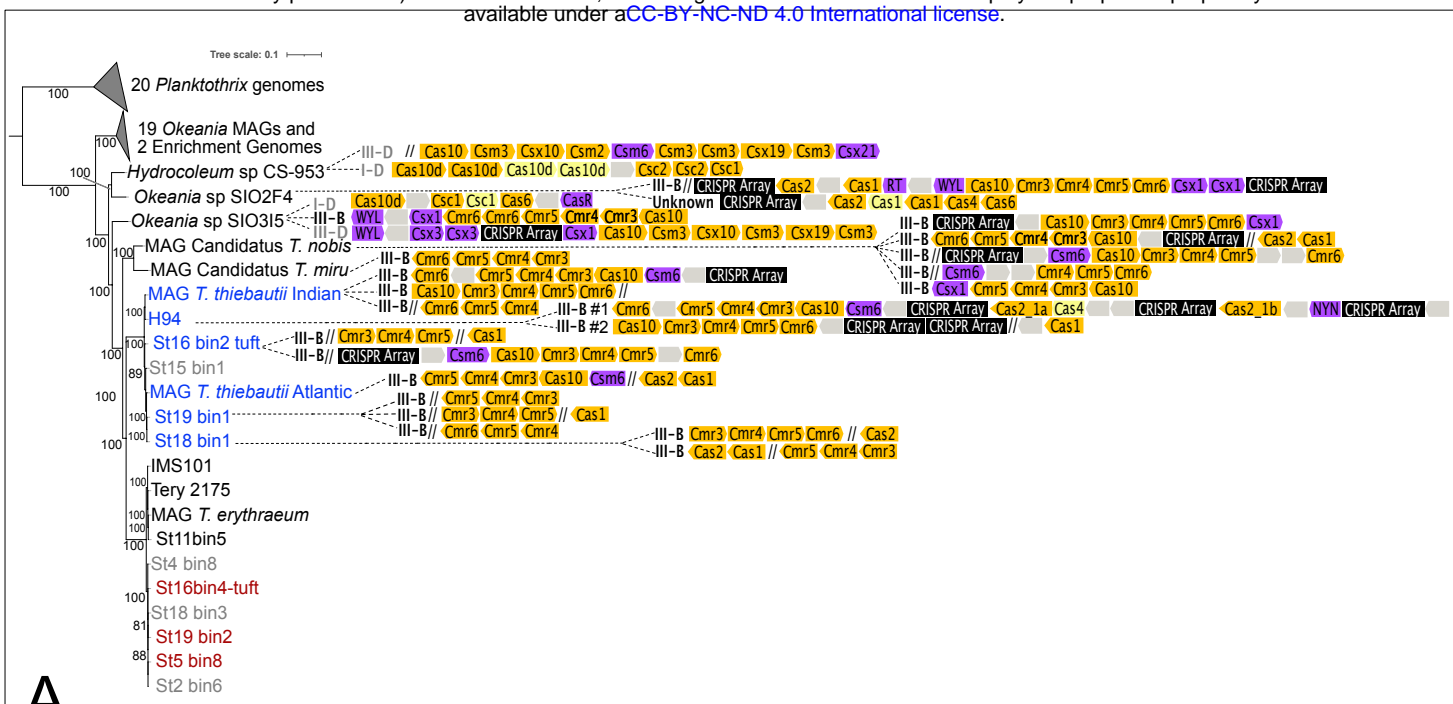


A

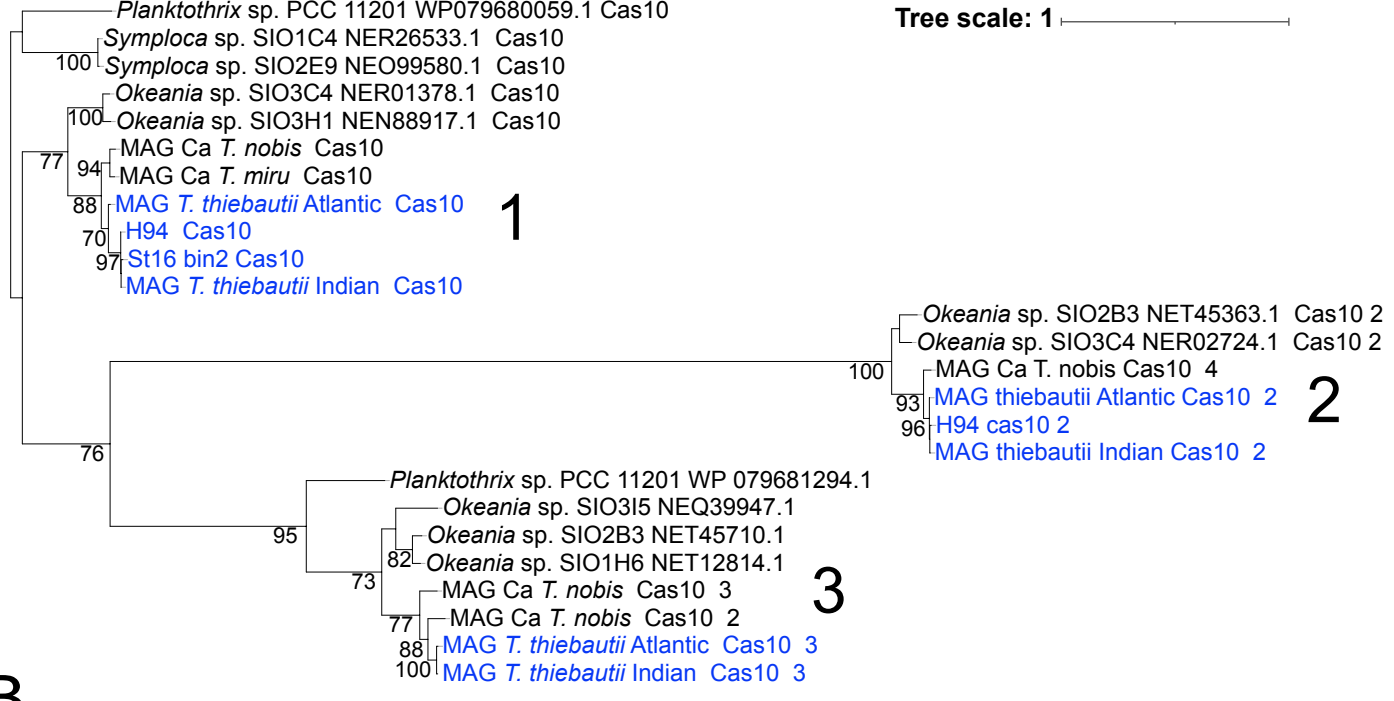


B





A



B

